Involvement of parvalbumin-positive neurons in the development of hyperalgesia in a mouse model of fibromyalgia
（線維筋痛症モデルマウスにおける痛覚過敏に脳内パルブアルブミン陽性ニューロンが関与する）

富山大学大学院 生命融合科学教育部
認知・情動脳科学専攻
システム情動科学講座

宮原　謙一郎

Abstract

Backgrounds: Fibromyalgia (FM) presents as chronic systemic pain, which might be ascribed to "central sensitization," in which pain information processing is amplified in the central nervous system. Since patients with FM display elevated gamma oscillations in the pain matrix and parvalbumin (PV)-positive neurons play a critical role in induction of gamma oscillations, we hypothesized that changes in PV-positive neurons are involved in hyperalgesia in fibromyalgia.
Methods: Mice received reserpine administration for 3 consecutive days as an animal model of FM (RES group), while control mice received vehicle injections in the same way (VEH group). The mice were subjected to hot-plate and forced swim tests, and immuno-stained PV-positive neurons were counted in the pain matrix. We investigated relationships between PV-positive neuron density in the pain matrix and pain avoidance behaviors.
Results: The mice in the RES group showed transient bodyweight loss and longer immobility time in the forced swim test than the mice in the VEH group. In the hot-plate test, the RES group showed shorter response latencies and a larger number of jumps in response to nociceptive thermal stimulus than the VEH group. Histological examination indicated an increase in the density of PV-positive neurons in the primary somatosensory cortex (S1) in the RES group. Furthermore, response latencies to the hot-plate were significantly and negatively correlated with the density of PV-positive neurons in the S1.
Conclusions: The results suggest a critical role for PV-positive neurons in the S1 to develop hyperalgesia in FM.

Keywords: fibromyalgia, mice, pain sensitivity, parvalbumin-positive neurons, reserpine, somatosensory cortex

Introduction

Fibromyalgia (FM) presents with chronic systemic pain along with psychotic (e.g., depression) and autonomic nervous symptoms (Wolfe et al., 1995; Carmona et al., 2001; Häuser et al., 2008; Bennett et al., 2007). Epidemiological studies of FM in various countries have reported an average prevalence of 2.7% (Makela et al., 1991; White et al., 1999; Wolfe et al., 2013; Queiroz, 2013). However, FM is refractory, and its pathophysiological mechanisms are not fully understood. Treatment methods of FM are under development, and various pharmacological therapies combined with non-pharmacological therapies have been used (Hughes et al., 2006; Macfarlane et al., 2017; Häuser and Fitzcharles, 2018; Borchers and Gershwin, 2015). Recently, "central sensitization," in which pain information processing is amplified in the central nervous system, has been suggested to play an essential role in FM (Woolf, 2011; Phillips and Clauw, 2013; Clauw, 2014).

Consistent with the above hypothesis, functional magnetic resonance imaging (fMRI) studies have reported hyperactivity in multiple brain areas that process pain, including the somatosensory area, prefrontal cortex, anterior cingulate cortex, and insula in response to mechanical, thermal and electrical stimulation in patients with FM as well as an animal model of FM (Gracely et al., 2002; Cook et al., 2004; Wells et al., 2017; Hubbard et al., 2020). Neurophysiological studies also reported that excitability in the primary somatosensory (S1) cortex was increased in patients with FM (Maetsu et al., 2013; Lim et al., 2015). Furthermore, gamma oscillations in S1 were correlated with subjective pain (or behavioral responses to nociceptive stimuli in rats) and/or physical stimulus intensity in intact humans and rats (Gross et al., 2007; Hauck et al., 2007; Schulz et al., 2011; Zhang et al., 2012; Peng et al., 2018; Heid et al., 2020). Gamma oscillations were elevated in the S1, motor cortex, insula, and prefrontal cortex in patients with FM compared with controls (Lim et al., 2016).

Several animal models of FM have been reported. Repeated injection of reserpine, which results in the depletion of monoamines in the nervous system, has been used as an animal model of FM (Nagakura et al., 2009; Uchida et al., 2019). In this model, the animals showed behaviors associated with pain (hyperalgesia and allodynia), depression-like symptoms, and gastrointestinal dysfunction (autonomic symptoms), which are all observed in human FM. Furthermore, reserpine administration increased the responses of

mechanoreceptive C-nociceptors and the activity of dorsal horn microglia in the spinal cord (Taguchi et al., 2015). These previous human and animal studies suggest that the forebrain pain matrix might be hyperactive to display complex FM symptoms. On the other hand, a recent animal study reported that optogenetic activation of parvalbumin (PV)-positive neurons in the S1 induced gamma oscillations of local field potentials and pain-related avoidance behaviors (Tan et al., 2019). Furthermore, optogenetic activation of PV-positive neurons in the prelimbic cortex also enhanced avoidance responses to nociceptive stimuli (Zhang et al., 2015). Based on these findings, we hypothesized that PV-positive neurons play an essential role in pain information processing in FM. In this study, we investigated the relationship between PV-positive neurons in the forebrain pain matrix and pain sensitivity in an animal model of FM with repeated reserpine administration.

Methods

Subjects

Eight to 10-week-old C57BL/6J male mice (n=60, Japan SLC, Hamamatsu, Japan) were used. The mice were housed in groups (four per cage) in a temperature-controlled experimental room (22 ± 1 °C) with light control (lights on from 07:00 to 19:00) and food and water available *ad libitum*. The mice were treated consistently with the guidelines for care and use of laboratory animals approved by the University of Toyama and the National Institutes of Health's Guide for the Care and Use of Laboratory Animals. The experimental protocol of the study was approved by the Animal Experiments and Ethics Committee at the University of Toyama (Permit No. A2016MED-2 3).

Animal model of FM by reserpine

An animal model of FM was produced using the protocol described in previous studies (Klein et al., 2014; de Souza et al., 2014; Taguchi et al., 2015). Reserpine (Nacalai Tesque, Inc., Kyoto, Japan), adjusted to a concentration of 0.25 mg/mL with 0.5% acetic acid, was injected (0.25 mg/kg, s.c.) into the back skin once a day for 3 successive days (RES group). As a control, a vehicle solution (0.5% acetic acid) was similarly injected (VEH group).

Behavioral tests

Hot-plate test

Behavioral responses to nociceptive thermal stimuli were observed 3 days after the first injection. We assessed thermal hyperalgesia using the hot-plate test. After placing each mouse on a hot-plate apparatus (Muromachi Kikai, Japan), the latency of behavioral responses [hindpaw licking or jumping (whichever came first)], and the number of jumps were measured. The surface temperature of the hot-plate was set at 50 ± 0.5 °C before testing, and the test was completed in 60 s to avoid tissue damage to the animals.

Forced swim test

Two different groups of mice underwent the forced swim test 3-4 and 10-11 days after the first injection to determine the depressive behaviors caused by reserpine. The procedures were conducted in accordance with those in Porsolt et al. (1978). Each mouse was placed in water (25±1 °C) in a glass beaker (23 cm × 35 cm × 20 cm; diameter × height × depth) for 15 min 3 or 10 days after the first injection. Twenty-four hours after the first forced swim test (i.e., 4 or 11 days after the first injection), the mice were again placed in the same glass beaker with water for 5 min, and their behavior was recorded by a video camera. The immobility time was measured for 5 min in the second forced swim test. Immobility was defined as the absence of any movement except that to keep the mouse's head above the water. After testing, the animals were towel-dried and returned to their cages.

Immunohistochemistry

PV-positive neurons were immunostained based on the same protocol used in our previous studies (Nguyen et al., 2011; Urakawa et al., 2013; Nakamura et al., 2015; Jargalsaikhan et al., 2017; Hongo et al., 2020). After the hot-plate test was performed 3 days after the first injection, the mice were sacrificed under deep anesthesia with mixed anesthetics (5.0 mg/kg butorphanol, 4.0 mg/kg midazolam, and 0.75 mg/kg medetomidine, i.p.), by transcardial perfusion with heparinized 0.01 M phosphate buffer saline (PBS), followed by 4% paraformaldehyde dissolved in 0.1 M phosphate buffer (PB). After perfusion, the brains were post-fixed in 4% paraformaldehyde overnight. The fixed brain was then immersed in 30% sucrose until they sank to the bottom. Then, the brains were cut into 40 μm sections, collected in 0.01 M PBS, and stored in an antifreeze solution (25% glycerin, 25% ethylene glycol, and 50% 0.1 M PB) at −20 °C. Two stains were used on serial sections every 40 μm, one for PV immunocytochemistry, and the other for Cresyl

violet (Nissl staining). In PV immunostaining, the sections were processed with mouse monoclonal anti-PV antibodies (1:10 000 dilution in 1% horse serum PBS, Sigma, St. Louis, MO, USA) according to our previous protocol.

Stereological analysis of PV-positive neurons

PV-positive neurons were counted based on our previous protocols (Nakamura et al., 2015; Jargalsaikhan et al., 2017; Hongo et al., 2020). Section images were captured and digitized using a microscope system (BZ-9000, Keyence Corporation, Osaka, Japan). Anatomical locations of the brain areas were determined by examining the anatomically matched adjacent Nissl-stained sections based on the brain atlas (Paxinos and Franklin, 2004); at +0.98, +0.62, +0.14, -0.34, -0.70, and -1.22 mm in the anterior-to-posterior level from the bregma in the primary somatosensory cortex (S1); at +1.98, +1.70, +1.42, +1.10 mm in the medial prefrontal cortex (mPFC) including the prelimbic cortex (PrL), infralimbic cortex (IL) and anterior cingulate cortex (ACC); at -0.82, -1.22, -1.58, -1.94, -2.30 mm in the lateral (LA) and basolateral (BLA) nuclei of the amygdala; at -0.82, -1.58 mm in the intercalated cells of the amygdala (ITC); at +0.38, -0.22, -0.82, -1.22 mm in the granular insula (GI), dysgranular insula (DI), and agranular insula (AI). In S1, both the forelimb (S1FL) and hindlimb (S1HL) regions were separately analyzed.

The PV-positive neurons were counted using stereological software (Stereo Investigator version 7.53.1, MicroBrightField, Williston, VT, USA). The counting conditions were as follows; sampling grid sizes, 280.87 × 765.50-μm in the mPFC, and 259.00 × 372.40-μm in the S1, amygdala, and insula; counting frame, 200 × 200-μm; optical dissector height, 5 μm. The PV-positive neuron density was estimated in each brain area of each animal.

Statistical analysis

Data were shown as the mean ± SEM. Normality of the data was checked by D'Agostino & Pearson test. The bodyweights were compared between the two groups using a repeated measures two-way analysis of variance (ANOVA) with posthoc tests (Bonferroni tests). In this analysis, the degrees of freedom were corrected by Greenhouse-Geisser method where appropriate. Data in the behavioral tests and PV-positive neuron density were compared between the VEH and RES groups using unpaired t-tests with Welch's correction (Welch's test) except the data in numbers of jumps in the hot-plate test, immobility time in

the forced swim test 11 days after the first injection, and PV-positive neuron density in the infralimbic cortex. The data in numbers of jumps in the hot-plate test, immobility time in the forced swim test 11 days after the first injection, and PV-positive neuron density in the infralimbic cortex were analyzed by the Mann-Whitney U test because these data did not show normal distribution. A linear regression analysis was used to analyze the relationship between the response latencies in the hot-plate test and PV-positive neuron density. Prism 8 (GraphPad Software Inc.) was used to analyze the data. A p-value of < 0.05 was considered statistically significant.

Results

General conditions of the reserpinized animals

The bodyweight of the RES group decreased after reserpine injection (Fig. 1). The statistical analysis indicated significant main effects of group [$F(1, 26)=5.54$, $p = 0.026$] and day [$F(2.82, 73.27)=49.22$, $p < 0.001$], and a significant interaction between group and day [$F(13, 338)=30.62$, $p < 0.0001$]. Post hoc comparisons indicated that the mean bodyweights were significantly smaller in the RES group than in the VEH group 3 days after the first injection (3d in Fig. 1; 22.3 ± 0.5 vs. 25.9 ± 0.4 g: mean ± SEM; Bonferroni test, $p < 0.0001$), 4 days after the first injection (4d in Fig. 1; 22.8 ± 0.6 vs. 25.9 ± 0.4 g; Bonferroni test, $p = 0.0046$), and 5 days after the first injection (5d in Fig. 1; 23.7 ± 0.5 vs. 26.0 ± 0.4 g; Bonferroni test, $p = 0.0248$).

Behavioral tests

Hot-plate test

The mice underwent the hot-plate test 3 days after the first injection (Fig. 1). The response latencies to nociceptive thermal stimuli were significantly shorter in the RES group (18.7 ± 1.2 s, n =16) than in the VEH group (35.9 ± 3.0 s, n = 16) (Welch's test, $p < 0.0001$; Fig. 2A). The number of jumps was significantly greater in the RES group (5.8 ± 1.6 times, n =16) than in the VEH group (0.0 ± 0.0 times, n = 16; Mann-Whitney U test, $p < 0.0001$; Fig. 2B). These results indicate that pain sensitivity was increased in the RES group.

Forced swim test

Figure 3 shows the immobility time four and eleven days after the first injection (Fig. 1). On day 4, the immobility time in the RES group (156.9 ± 19.9 s, n = 8) tended to be longer than that in the VEH group (109.3 ± 17.7 s, n = 8; Welch's test, p = 0.0967; Fig. 3A). On day 11, the immobility time was significantly longer in the RES group (202.8 ± 12.1 s, n = 6) than in the VEH group (155.1 ± 8.9 s, n = 6; Mann-Whitney U test, p = 0.0152; Fig. 3B).

PV-positive neuron density

Example microphotographs of PV-positive neurons in S1 for the VEH and RES groups are shown in Fig. 4. The number of PV-positive neurons was greater in the RES group than in the VEH group. Figure 5 shows PV-positive neuron density (cells/mm^3) in the S1 forelimb (S1FL) (A) and S1 hindlimb (S1HL) regions (B), and cell density in the S1L (mean cell density between the S1FL and S1HL) (C). The Welch's test indicated that PV-positive neuron density was significantly greater in the RES group than in the VEH group in each area (S1FL, p = 0.0002; S1HL, p = 0.0004; S1L, p = 0.0002). However, in the other brain regions, including the mPFC (PrL, IL, and ACC), amygdala (LA, BLA, and ITC), and insula (GI, DI, and AI), no significant differences were observed between the VEH and RES groups (Supplementary Fig. 1).

Correlation analyses

The relationships between PV-positive neuron density and behavioral manifestation of thermal hyperalgesia (response latency) were analyzed in each brain area. The response latencies in the hot-plate test were significantly negatively correlated with cell density in the S1FL [r = -0.680; F(1, 18) = 15.50, p = 0.001; Fig. 6A], S1HL [r = -0.645; F(1, 18) = 12.80, p = 0.002; Fig. 6B], and S1L [r = -0.677; F(1, 18) = 15.19, p = 0.001; Fig. 6C]. In the other brain regions, including the mPFC (PrL, IL, and ACC), amygdala (LA, BLA, and ITC), and insula (GI, DI, and AI), no such relationships were observed (Supplementary Figs. 2 and 3).

Discussion

Reproduction of the FM model

A previous study reported that the metabolites of serotonin, dopamine, and

noradrenaline in the cerebrospinal fluid (CSF) were lower in patients with FM, suggesting that catecholamine levels may be lower in the brain (Russel et al., 1992). Consistently, the animal model of FM with repeated reserpine administration replicated human FM symptoms and displayed decreases in catecholamines in the brain and spinal cord (Nagakura et al., 2009, 2018; Oe et al., 2010; Klein et al., 2014; de Souza et al., 2014). The present study also replicated characteristic symptoms of human patients with FM and the animal model of FM reported in previous studies. First, patients with FM often present with eating disorders and/or bodyweight loss (Miyamae et al., 2016; López-Rodríguez et al., 2017). Previous animal studies also reported that the FM mouse model displayed the lowest bodyweight 3 days after the first injection (Taguchi et al., 2015; Nagakura et al., 2018). After the reserpine administration, access to food was reduced, eating time was extended, and food intake was sharply reduced (Serra et al., 2015). In the present study, the RES group also showed a decrease in bodyweight 3-5 days after the first injection.

Second, previous studies reported that reserpine-induced changes in pain sensation include mechanical hyperalgesia of the skin and muscles and thermal hyperalgesia. A single dose of reserpine (4 to 5 mg/kg) was found to cause skin and muscle hyperalgesia several hours after injection, and transiently induced thermal hyperalgesia (Kulkarni and Robert, 1982; Matsumoto et al., 1996). Repeated administration of reserpine resulted in a decrease in the escape threshold for mechanical stimulation of skin and muscle 3 to 14 days after the first injection, while a decrease in escape latency to thermal stimulation was observed 3 to 4 days after the first injection (Klein et al., 2014; de Souza et al., 2014; Oe et al., 2010). The present results, in which significant thermal hyperalgesia in the hot-plate test was observed 3 days after the first injection, were consistent with those of previous studies.

Third, depression is an important characteristic of human FM, and the same pathophysiological mechanisms may be involved in both depression and changes in pain sensitivity (Gracely et al., 2012; Thiagarajah et al., 2014). Depression-like symptoms (i.e., immobility in the forced swim test) were not observed 3 days after the first injection of reserpine but were observed 5-14 days after the first injection (Nagakura et al., 2009; Klein et al., 2014; de Souza et al., 2014). Consistently, the immobility time tended to increase 4 days after the first injection and was significantly increased 11 days after the first injection in the RES group. These findings indicate that the present study replicated the symptoms of the FM model with repeated reserpine administration.

Relationship between PV-positive neuron density and hyperalgesia

In this study, repeated reserpine administration increased PV-positive neuron density in S1, and there was a negative correlation between PV-positive neuron density and behavioral latency in the hot-plate test. Previous studies reported that optogenetic activation of fast-spike PV-positive neurons controlled pyramidal neuron activity and generated gamma oscillations above 40 Hz (Bartos et al., 2007; Sohal et al., 2009; Cardin et al., 2009). Consistently, optogenetic activation of PV-positive neurons in the S1 induced gamma oscillations (Tan et al., 2019). Since gamma oscillations in S1 were correlated with behavioral responses to nociceptive stimuli and gamma oscillations were elevated in S1 in patients with FM (see Introduction), the present results with elevated PV-positive neuron density in S1 and decreases in response latencies in the hot-plate test strongly suggest increased gamma oscillations in the RES group.

Optogenetic activation of PV-positive neurons in S1 not only increased behavioral sensitivity to nociceptive stimuli but also markedly increased activity of the rostroventral medulla (RVM), which functions as the descending pain modulatory system (Tan et al., 2019). It has been demonstrated that the periaqueductal gray (PAG) and RVM in the midbrain regulate nociceptive inputs (Reynolds, 1969; Hosobuchi et al., 1977; Heinricher et al., 2009; Ossipov et al., 2010; Mills et al., 2018). ON and OFF cells are mixed in the RVM. Nociceptive information processing is suppressed by the activity of OFF cells, whereas it is promoted by the activity of ON cells (Fields et al., 1995; Felice et al., 2011; Mason, 2012). In an FM model with reserpine administration, mechanoreceptive C nociceptor responses and activity of dorsal horn microglia in the spinal cord were increased (Taguchi et al., 2015), and activated microglia might disinhibit dorsal horn nociceptive neurons (Beggs and Salter, 2010). Along with the reduction of descending pain-inhibitory catecholaminergic inputs to the spinal cord by reserpine (Nagakura et al., 2009; Taguchi et al., 2015), activation of PV-positive neurons in S1 might promote the activity of ON cells in the RVM, most of which might be non-serotonergic (Marinelli et al., 2002), to further amplify pain information processing in the dorsal horn. These findings further suggest that the S1 and dorsal horn might form positive feedback neural circuits to amplify pain sensory information processing.

On the other hand, human fMRI studies reported increased activity in the prefrontal cortex, anterior cingulate, amygdala, and insula at rest and in response to heat noxious stimuli in patients with FM (McLoughlin et al., 2011; Ellingson et al., 2012; Kim et al., 2013). The size of the amygdala changes in patients with FM (Burgmer et al., 2009; Cifre et

al., 2012; Lutz et al., 2008). However, PV-positive neuron density did not change in these brain regions in the present study. These findings suggest that pathological alterations in PV-positive neurons specifically occur in S1 in an animal model of FM with repeated reserpine administration. However, in the present study, reserpine was administered for only three consecutive days, suggesting that the present results might reflect acute effects. A larger number of reserpine injections would induce changes in other brain regions since sustained changes in catecholamine levels are critical to inducing hyperalgesia (Oe et al., 2010). Furthermore, in the present study, the animals were sacrificed 3 days after the first injection. Therefore, it is also possible that a longer duration after the first injection might be required to induce changes in PV-positive neurons in other brain regions. Further studies are required to confirm the S1 specificity of PV-positive neuronal changes in FM.

Possible pathophysiological mechanisms of FM by reserpine

A previous clinical study reported decreases in catecholamine metabolites in the CSF in FM patients, but no alteration of those levels in patients with rheumatoid arthritis, suggesting that alteration of catecholamine metabolites is a cause, but not a consequence, of chronic pain (Russel et al., 1992). Previous studies reported that catecholamines in the brain suppressed gamma oscillations, whereas their depletion increased gamma oscillations. Dopamine controls gamma oscillations differently depending on its receptor type (Furth et al., 2013). However, gross depletion of dopamine by pharmacological lesions of dopaminergic terminals in the striatum was found to increase gamma oscillations (Lemaire et al., 2012). Furthermore, dopamine reduced gamma oscillation through the α1-adrenergic receptor in the primary motor cortex (Özkan et al., 2017). In addition, electrical stimulation of the dorsal raphe nucleus to release serotonin downregulated cortical gamma oscillation (Puig et al., 2010), while pharmacological stimulation of the locus coeruleus to release noradrenalin reduced gamma oscillation in the dentate gyrus (Brown et al., 2005). Another line of evidence also indicated an involvement of reserpine in induction of gamma oscillations: reserpine injections increased rapid eye movement (REM) sleep (Blasco-Serra et al., 2020), in which gamma oscillations increased compared with non-REM sleep (Scheffzük et al., 2011). On the other hand, pregabalin, an antagonist of voltage-dependent Ca^{2+} channels (VDCCs), is reported to be effective in treating FM (Verma et al., 2014). VDCCs are reported to be critical for gamma oscillations in the thalamocortical system (Llinás et al., 2007). All of these findings support the critical role of gamma oscillation in

pain information processing in the forebrain of FM. Gamma oscillation is reported to induce synaptic plasticity (Zarnadze et al., 2016; Park et al., 2020), by which pain sensory circuits might be strengthened in FM. Alteration of PV-positive neurons in the present study may reflect these pathological changes induced by reserpine.

References

Bartos, M., Vida, I., Jonas, P. (2007). Synaptic mechanisms of synchronized gamma oscillations in inhibitory interneuron networks. Nat. Rev. Neurosci, 8, 45–56. doi: 10.1038/nrn2044

Beggs, S., Salter, M. W. (2010). Microglia-neuronal signaling in neuropathic pain hypersensitivity 2.0. Curr Opin Neurobiol, 20, 474-480. doi: 10.1016/j.conb.2010.08.005

Bennett, R. M., Jones, J., Turk, D. C., Russell, I. J., & Matallana, L. (2007). An internet survey of 2,596 people with fibromyalgia. BMC Musculoskelet. Disord, 8, 27. doi: 10.1186/1471-2474-8-27

Blasco-Serra, A., Alfosea-Cuadrado, G., Cervera-Ferri, A., González-Soler, E. M., Lloret A, Martínez-Ricós, J., Teruel-Martí, V., Valverde-Navarro, A.A. (2020). Hippocampal oscillatory dynamics and sleep atonia are altered in an animal model of fibromyalgia: Implications in the search for biomarkers. J Comp Neurol, 528, 1367-1391. doi: 10.1002/cne.24829

Borchers, A. T., & Gershwin, M. E. (2015). Fibromyalgia: A Critical and Comprehensive Review. Clinical Reviews in Allergy & Immunology, 49, 100–151. doi: 10.1007/s12016-015-8509-4

Brown, R. A., Walling, S. G., Milway, J.S., Harley, C. W. (2005). Locus ceruleus activation suppresses feedforward interneurons and reduces beta-gamma electroencephalogram frequencies while it enhances theta frequencies in rat dentate gyrus. J Neurosci, 25, 1985-1991. doi:10.1523/JNEUROSCI.4307-04.2005

Burgmer, M., Gaubitz, M., Konrad, C., Wrenger, M., Hilgart, S., Heuft, G., Pfleiderer, B. (2009). Decreased gray matter volumes in the cingulo-frontal cortex and the amygdala in patients with fibromyalgia. Psychosomatic Medicine, 71, 566-573. doi: 10.1097/PSY.0b013e3181a32da0

Carmona, L., Ballina, J., Gabriel, R., Laffon, A. (2001). The burden of musculoskeletal

diseases in the general population of Spain: results from a national survey. Annals of Rheumatic Diseases. 60, 1040-1045. doi: 10.1136/ard.60.11.1040

Cardin, J. A., Carlén, M., Meletis, K., Knoblich, U., Zhang, F., Deisseroth, K., Tsai, L. H., Moore, C. I. (2009). Driving fast-spiking cells induces gamma rhythm and controls sensory responses. Nature, 459, 663–668. doi: 10.1038/nature08002

Cifre, I., Sitges, C., Fraiman, D., Muñoz, M. Á., Balenzuela, P., González-Roldán, A., Martínez-Jauand, M., Birbaumer, N., Chialvo, D. R., Montoya, P. (2012). Disrupted functional connectivity of the pain network in fibromyalgia. Psychosom Med, 74, 55–62. doi: 10.1097/PSY.0b013e3182408f04

Clauw, D. J. (2014). Fibromyalgia: a clinical review. JAMA, 311, 1547–1555. doi:10.1001/jama.2014.3266

Cook, D. B., Lange, G., Ciccone, D. S., Liu, W. C., Steffener, J., Natelson, B. H. (2004). Functional imaging of pain in patients with primary fibromyalgia. J Rheumatol, 31, 364-378.

de Souza, A. H., da Costa Lopes, A. M., Castro, C. J. jr., Pereira, E. M., Klein, C. P., da Silva, C. A. Jr., da Silva, J. F., Ferreira, J., Gomez, M. V. (2014). The effects of Phα1β, a spider toxin, calcium channel blocker, in a mouse fibromyalgia model. Toxicon, 81, 37-42. doi:10.1016/j. toxicon.2014.01.015

Ellingson, L. D., Shields, M. R., Stegner, A. J., Cook, D. B. (2012). Physical activity, sustained sedentary behavior, and pain modulation in women with fibromyalgia. Journal of Pain, 13, 195-206. doi: 10.1016/j.jpain.2011.11.001

Felice, M. D., Wang, R. S. R., Portocarrero, L. V., Oyarzo, J., King, T., Ossipov, M. H., Vanderah, T. W., Lai, J., Dussor, G. O., Fields, H. L., Price, T. J., Porreca, F. (2011). Engagement of descending inhibition from the rostral ventromedial medulla protects against chronic neuropathic pain. Pain, 152, 2701-2709. doi: 10.1016/j.pain.2011.06.008

Fields, H. L., Malick, A., Burstein, R. (1995). Dorsal horn projection targets of ON and OFF cells in the rostral ventromedial medulla. J Neurophysiol, 74, 1742-1759. doi: 10.1152/jn. 1995.74.4.1742

Furth, K. E., Mastwal, S., Wang, K. H., Buonanno, A., Vullhorst, D. (2013). Dopamine, cognitive function, and gamma oscillations: role of D4 receptors. Front Cell Neurosci, 7, 102. doi: 10.3389/fncel.2013.00102

Gracely, R. H., Petzke, F., Wolf, J. M., Clauw, D. J. (2002). Functional magnetic resonance imaging evidence of augmented pain processing in fibromyalgia. Arthritis Rheum, 46,

1333-1343. doi: 10.1002/art.10225

Gracely, R. H., Ceko, M, and Bushnell, M. C. (2012). Fibromyalgia and depression. Pain Res Treat, 2012, 486590. doi: 10.1155/2012/486590

Gross, J., Schnitzler, A., Timmermann, L., Ploner, M. (2007). Gamma oscillations in human primary somatosensory cortex reflect pain perception. PLOS Biology, 5, e133. doi: 10.1371/journal.pbio.0050133

Hauck, M., Lorenz, J., Engel, A. K. (2007). Attention to painful stimulation enhances gamma-band activity and synchronization in human sensorimotor cortex. J Neurosci, 27, 9270–9277. doi: 10.1523/JNEUROSCI.2283-07.2007

Häuser, W., Fitzcharles, M. A. (2018). Facts and myths pertaining to fibromyalgia. Dialogues Clin Neurosci, 20, 53-62.

Häuser, W., Zimmer, C., Felde, E., Köllner, V. (2008). What are the key symptoms of fibromyalgia? Results of a survey of the German Fibromyalgia Association. Schmerz, 22, 176-183. doi: 10.1007/s00482-007-0602-z

Heinricher, M. M., Tavares, I., Leith, J. L., Lumb, B. M. (2009). Descending control of nociception: specificity, recruitment and plasticity. Brain Res Rev, 60, 214–225. doi: 10.1016/ j.brainresrev.2008.12.009

Heid, C., Mouraux, A., Treede, R. D., Hofer, S. S., Rupp, A., Baumgärtner, U. (2020). Early gamma-oscillations as correlate of localized nociceptive processing in primary sensorimotor cortex. J Neurophysiol, 123, 1711-1726. doi: 10.1152/jn.00444.2019

Hongo, N., Takamura, Y., Nishimaru, H., Matsumoto, J., Tobe, K., Saito, T., Saido, T. C., Nishijo, H. (2020). Astaxanthin Ameliorated Parvalbumin-Positive Neuron Deficits and Alzheimer's Disease-Related Pathological Progression in the Hippocampus of App NL-G-F/NL-G-F Mice. Front Pharmacol, 11, 307. doi: 10.3389/fphar.2020.00307

Hosobuchi, Y., Adams, J. E., Linchitz, R. (1977). Pain relief by electrical stimulation of the central gray matter in humans and its reversal by naloxone. Science, 197, 183-186. doi: 10.1126/science.301658

Hubbard, C. S., Lazaridou, A., Cahalan, C. M., Kim, J., Edwards, R. R., Napadow, V., Loggia, M. L. (2020). Aberrant salience? Brain hyperactivation in response to pain onset and offset in fibromyalgia. Arthritis Rheumatol, 72, 1203-1213. doi: 10.1002/art.41220

Hughes, G., Martinez, C., Myon, E., Taïeb, C., Wessely, S. (2006). The impact of a diagnosis of fibromyalgia on health care resource use by primary care patients in the UK: An observational study based on clinical practice. Arthritis Rheum, 54, 177-183. doi:

10.1002/art.21545

Jargalsaikhan, U., Nishimaru, H., Matsumoto, J., Takamura, Y., Nakamura, T., Hori, E., Kondoh, T., Ono, T., Nishijo, H. (2017). Ingestion of dried-bonito broth (dashi) facilitates PV-parvalbuminimmunoreactive neurons in the brain, and affects emotional behaviors in mice. Nutr. Neurosci, 20, 571–586. doi: 10.1080/1028415X.2016.1208429

Kim, J. Y., Kim, S., Seo, J., Kim, S. H., Han, S. W., Nam, E. J., Kim, S. K., Lee, H. J., Lee S. J., Kim, Y. T., Chang, Y. (2013). Increased power spectral density in resting-state pain-related brain networks in fibromyalgia. Pain, 154, 1792-1797. doi: 10.1016/j.pain.2013.05.040

Klein, C. P., Sperotto, N. D., Maciel, I. S., Leite, C. E., Souza, A. H., Campos, M. M. (2014). Effects of d-series Resolvins on behavioral and neurochemical changes in a fibromyalgia-like model in mice. Neuropharmacology, 86, 57-66. doi: 10.1016/j.neuropharm.2014.05.043

Kulkarni, S. K., Robert, R. K. (1982). Reversal by serotonergic agents of reserpine-induced hyperalgesia in rats. Eur J Pharmacol, 83, 325-328. doi: 10.1016/0014-2999(82)90271-0

Lemaire, N., Hernandez, L. F., Hu, D., Kubota, Y., Howe, M. W., Graybiel, A. M. (2012). Effects of dopamine depletion on LFP oscillations in striatum are task- and learning-dependent and selectively reversed by L-DOPA. Proc Natl Acad Sci U S A, 109, 18126-18131. doi: 10.1073/pnas.1216403109

Lim, M., Roosink, M., Kim, J. S., Kim, D. J., Kim, H. W., Lee, E. B., Kim, H. A., Chung, C. K. (2015). Disinhibition of the primary somatosensory cortex in patients with fibromyalgia. Pain, 156, 666-74. doi: 10.1097/j.pain.0000000000000096

Lim, M., Kim, J. S., Kim, D. J., and Chung, C. K. (2016). Increased low- and high-frequency oscillatory activity in the prefrontal cortex of fibromyalgia patients. Front Hum Neurosci, 10, 1-11. doi: 10.3389/fnhum.2016.00111

Llinás, R. R., Choi, S., Urbano, F. J., Shin, H. S. (2007). Gamma-band deficiency and abnormal thalamocortical activity in P/Q-type channel mutant mice. Proc Natl Acad Sci U S A, 104, 17819-17824. doi: 10.1073/pnas.0707945104

López-Rodríguez, M. M., Molina, J. G., Medina, I. M. F., Sola, C. F., Muelle, A. R. (2017). Patterns of food avoidance and eating behavior in women with fibromyalgia. Endocrinol Diabetes Nutr, 64, 480-490. doi: 10.1016/j.endinu.2017.07.002

Lutz, J., Jäger, L., de Quervain, D., Krauseneck, T., Padberg, F., Wichnalek, M., Beyer, A., Stahl, R., Zirngibl, B., Morhard, D., Reiser, M., Schelling, G. (2008). White and gray

matter abnormalities in the brain of patients with fibromyalgia: a diffusion-tensor and volumetric imaging study. Arthritis & Rheumatology, 58, 3960-3969. doi: 10.1002/art. 24070

Macfarlane, G. J., Kronisch, C., Dean, L. E., Atzeni, F., Häuser, W., Fluß, E., Choy, E., Kosek, E., Amris, K., Branco, J., Dincer, F., Leino-Arjas, P., Longley, K., McCarthy, G. M., Makri, S., Perrot, S., Sarzi-Puttini, P., Taylor, A., Jones, G. T. (2017). EULAR revised recommendations for the management of fibromyalgia. Ann Rheum Dis, 76, 318-328. doi: 10.1136/annrheumdis-2016-209724

Makela. M., Heliovaara, M. (1991). Prevalence of primary fibromyalgia in the Finnish population. British Medical Journal, 303, 216-219. doi: 10.1136/bmj. 303.6796.216

Marinelli, S., Vaughan, C. W., Schnell, S. A., Wessendorf, M. W., Christie, M. J. (2002). Rostral ventromedial medulla neurons that project to the spinal cord express multiple opioid receptor phenotypes. J Neurosci, 22, 10847-10855. doi:10.1523/JNEUROSCI.22-24-10847.2002

Mason, P. (2012). Medullary circuits for nociceptive modulation. Curr Opin Neurobiol, 22, 640–645. doi: 10.1016/j.conb.2012.03.008

Matsumoto, M., Mizowaki, M., Suchitra, T., Murakami, Y., Takayama, H., Sakai, S., Aimi, N., Watanabe, H. (1996). Central antinociceptive effects of mitragynine in mice: contribution of descending noradrenergic and serotonergic systems. Eur J Pharmacol, 317, 75-81. doi: 10.1016/s0014-2999(96)00714-5

McLoughlin, M. J., Stegner, A. J., Cook, D. B. (2011). The relationship between physical activity and brain responses to pain in fibromyalgia. Journal of Pain, 12, 640-51. doi: 10.1016/j.jpain.2010.12.004

Maestu, C., Cortes, A., Vazquez, J. M., del Rio, D., Gomez-Arguelles, J. M., del Pozo, F., Nevado, A. (2013). Increased brain responses during subjectively-matched mechanical pain stimulation in fibromyalgia patients as evidenced by MEG. Clin Neurophysiol, 124, 752-60. doi: 10.1016/j.clinph.2012.09.015

Mills, E. P., Di Pietro, F., Alshelh, Z., Peck, C. C., Murray, G. M., Vickers, E. R., Henderson, L. A. (2018). Brainstem pain-control circuitry connectivity in chronic neuropathic pain. J Neurosci, 38, 465-473. doi: 10.1523/JNEUROSCI.1647-17.2017

Miyamae, T., Isozaki, J., Kikuchi, M., Yokota, S. (2016). Eating disorder in juvenile fibromyalgia. J Child Adolesc Psychopharmacol. 26, 653-5. doi: 10.1089/cap.2014.0136

Nagakura, Y., Oe, T., Aoki, T., Matsuoka, N. (2009). Biogenic amine depletion causes

chronic muscular pain and tactile allodynia accompanied by depression: A putative animal model of fibromyalgia. Pain, 146, 26-33. doi: 10.1016/j.pain.2009.05.024

Nagakura, Y., Ohsaka, N., Azuma, R., Takahashi, S., Takebayashi, Y., Kawasaki, S., Murai S., Miwa, M., Saito, H. (2018). Monoamine system disruption induces functional somatic syndromes associated symptomatology in mice. Physiol Behav, 194, 505-514. doi: 10.1016/j.physbeh.2018.07.007

Nakamura, T., Matsumoto, J., Takamura, Y., Ishii, Y., Sasahara, M., Ono, T., Nishijo, H. (2015). Relationships among parvalbumin-immunoreactive neuron density, phase-locked gamma oscillations, and autistic/schizophrenic symptoms in PDGFR-ß knock-out and control mice. PloS One, 10, e0119258. doi: 10.1371/journal.pone.0119258

Nguyen, P. T., Nakamura, T., Hori, E., Urakawa, S., Uwano, T., Zhao, J., Li, R., Nguyen, D. B., Hamashima, T., Ishii, Y., Matsushima, T., Ono, T., Sasahara, M., Nishijo, H. (2011). Cognitive and socio-emotional deficits in platelet-derived growth factor receptor-ß gene knockout mice. PloS One, 6, e18004. doi: 10.1371/journal.pone.0018004

Oe, T., Tsukamoto, M., Nagakura, Y. (2010). Reserpine causes biphasic nociceptive sensitivity alteration in conjunction with brain biogenic amine tones in rats. Neuroscience, 169, 1860-1871. doi: 10.1016/j.neuroscience.2010.06.061

Ossipov, M. H., Dussor, G. O., Porreca, F. (2010). Central modulation of pain. J Clin Invest 120:3779–3787. doi: 10.1172/JCI43766

Özkan, M., Johnson, N. W., Sehirli, U. S., Woodhall, G. L., Stanford, I. M. (2017). Dopamine acting at D1-like, D2-like and α1-adrenergic receptors differentially modulates theta and gamma oscillatory activity in primary motor cortex. PLoS One, 12, e0181633. doi: 10.1371/ journal.pone.0181633

Park, K., Lee, J., Jang, H. J., Richards, B. A., Kohl, M. M., Kwag, J. (2020). Optogenetic activation of parvalbumin and somatostatin interneurons selectively restores theta-nested gamma oscillations and oscillation-induced spike timing-dependent long-term potentiation impaired by amyloid β oligomers. BMC Biol, 18, 7. doi: 10.1186/s12915-019-0732-7

Paxinos, G., Franklin, K. B. J. (2004). The Mouse Brain in Stereotaxic Coordinates. Second Edition. Gulf Professional Publishing; 2004.

Peng, W., Xia, X., Yi, M., Huang, G., Zhang, Z., Iannetti, G., Hu, L. (2018). Brain oscillations reflecting pain-related behavior in freely moving rats. Pain, 159, 106-118. doi: 10.1097/j.pain.0000000000001069

Phillips, K., Clauw, D. J. (2013). Central pain mechanisms in the rheumatic diseases: future directions. Arthritis Rheum. 65, 291-302. doi: 10.1002/art.37739

Porsolt, R. D., Bertin, A., Jalfre, M. (1978). "Behavioural despair" in rats and mice: strain differences and the effects of imipramine. Eur J Pharmacol, 51, 291-294. doi: 10.1016/ 0014-2999(78)90414-4

Puig, M. V., Watakabe, A., Ushimaru, M., Yamamori, T., Kawaguchi, Y. (2010). Serotonin modulates fast-spiking interneuron and synchronous activity in the rat prefrontal cortex through 5-HT1A and 5-HT2A receptors. J Neurosci, 30, 2211-2222. doi: 10.1523/JNEUROSCI. 3335-09.2010

Queiroz, L. P. (2013). Worldwide epidemiology of fibromyalgia. Curr Pain Headache Rep, 17, 356. doi: 10.1007/s11916-013-0356-5

Reynolds, D. V. (1969). Surgery in the rat during electrical analgesia induced by focal brain stimulation. Science, 164, 444-445. doi: 10.1126/science.164.3878.444

Russell, I. J., Vaeroy, H., Javors, M., Nyberg, F. (1992). Cerebrospinal fluid biogenic amine metabolites in fibromyalgia/fibrositis syndrome and rheumatoid arthritis. Arthritis Rheum. 35(5):550-6. doi: 10.1002/art.1780350509

Scheffzük, C., Kukushka, V. I., Vyssotski, A.L., Draguhn, A., Tort, A. B., Brankačk, J. (2011). Selective coupling between theta phase and neocortical fast gamma oscillations during REM-sleep in mice. PLoS One, 6, e28489. doi:10.1371/journal.pone.0028489

Schulz, E., Tiemann, L., Schuster, T., Gross, J., Ploner, M. (2011). Neurophysiological coding of traits and states in the perception of pain. Cereb Cortex, 21, 2408–2414. doi: 10.1093/ cercor/bhr027.

Serra, A. B., Vidal, F. E., Soler, E. M. G., Expósito, F. M., Ausina, M. C. B., Bellver, S. M., Ferri, A. C., Martí, V. T., Navarro, A. A. V. (2015). Depressive-like symptoms in a reserpine-induced model of fibromyalgia in rats. Physiol Behav, 151, 456–462. doi: 10.1016/j.physbeh.2015.07.033

Sohal, V, S., Zhang, F., Yizhar, O., Deisseroth, K. (2009). Parvalbumin neurons and gamma rhythms enhance cortical circuit performance. Nature, 459, 698–702. doi: 10.1038/nature07991

Taguchi, T., Katanosaka, K., Yasui, M., Hayashi, K., Yamashita, M., Wakatsuki, K., Kiyama, H., Yamanaka, A., Mizumura, K. (2015). Peripheral and spinal mechanisms of nociception in a rat reserpine-induced pain model. Pain, 156, 415–427. doi: 10.1097/01.j.pain.0000460334.49525.5e

Tan, L. L., Oswald, M. J., Heinl, C., Romero, O. A. R., Kaushalya, S. K., Monyer, H., Kune, R. (2019). Gamma oscillations in somatosensory cortex recruit prefrontal and descending serotonergic pathways in aversion and nociception. Nat Commun, 10, 983. doi: 10.1038/s41467-019-08873-z

Thiagarajah, A. S., Guymer, E, K., Leech, M., and Littlejohn, G. O. (2014). The relationship between fibromyalgia, stress and depression. Int. J. Clin. Rheumatol, 9, 371–384.

Uchida, M., Kobayashi, O., Yoshida, M., Miwa, M., Miura, R., Saito, H., Nagakura, Y. (2019). Coexistence of alterations of gastrointestinal function and mechanical allodynia in the reserpine-induced animal model of fibromyalgia. Dig Dis Sci, 64, 2538-2547. doi: 10.1007/s10620-019-05577-8

Urakawa, S., Takamoto, K., Hori, E., Sakai, N., Ono, T., Nishijo, H. (2013). Rearing in enriched environment increases parvalbumin-positive small neurons in the amygdala and decreases anxiety-like behavior of male rats. BMC Neurosci, 14, 13. doi: 10.1186/1471-2202-14-13

Verma, V., Singh, N., Jaggi A. S. (2014). Pregabalin in neuropathic pain: evidences and possible mechanisms. Curr Neuropharmacol, 12, 44-56. doi: 10.2174/ 1570159X1201140117162802

Wells, J. A., Shibata, S., Fujikawa, A., Takahashi, M., Saga, T., Aoki, I. (2017). Functional MRI of the Reserpine-Induced Putative Rat Model of Fibromyalgia Reveals Discriminatory Patterns of Functional Augmentation to Acute Nociceptive Stimuli. Sci Rep, 7, 38325. doi: 10.1038/srep38325

White, K. P., Speechley, M., Harth, M., Ostbye, T. (1999). The London Fibromyalgia Epidemiology Study: the prevalence of fibromyalgia syndrome in London. Ontario Journal of Rheumatology, 26, 1570-1576.

Wolfe, F., Ross, K., Anderson, J., Russell, I. J., Hebert, L. (1995). The prevalence and characteristics of fibromyalgia in the general population. Arthritis Rheum, 38, 19-28. doi: 10.1002/ art.1780380104

Wolfe, F., Brähler, E., Hinz, A., Häuser, W. (2013). Fibromyalgia prevalence, somatic symptom reporting, and the dimensionality of polysymptomatic distress: results from a survey of the general population. Arthritis Care Res (Hoboken), 65, 777–785. doi: 10.1002/acr. 21931

Woolf, C. J. (2011). Central sensitization: Implications for the diagnosis and treatment of pain. Pain, 152 (3 Suppl), S2-15. doi: 10.1016/j.pain.2010.09.030

Zarnadze, S., Bäuerle, P., Santos-Torres, J., Böhm, C., Schmitz, D., Geiger, J. R., Dugladze, T., Gloveli, T. (2016). Cell-specific synaptic plasticity induced by network oscillations. eLife, 5, e14912. doi: 10.7554/eLife.14912

Zhang, Z. G., Hu, L., Hung, Y. S., Mouraux, A., Iannetti, G. D. (2012). Gamma-band oscillations in the primary somatosensory cortex—a direct and obligatory correlate of subjective pain intensity. J Neurosci, 32, 7429-7438. doi: 10.1523/JNEUROSCI.5877-11.2012

Zhang, Z., Gadotti, V. M., Chen, L., Souza, I. A., Stemkowski, P. L., Zamponi, G. W. (2015). Role of prelimbic GABAergic circuits in sensory and emotional aspects of neuropathic pain. Cell Reports, 12, 752-759. doi: 10.1016/j.celrep.2015.07.001

Figure legends

Fig. 1. Time course of bodyweight.

The mean bodyweights were significantly lower in the RES group than in the VEH group 3-5 days after the first injection (3d, 4d, and 5d). ****, **, *, significant differences from the VEH group (Bonferroni test, $p < 0.0001$, 0.001, and 0.05, respectively). The arrows indicate reserpine or vehicle injection. Open circles, VEH group; filled circles, RES group. BL1-3, day 1-3 in the baseline period; 1-11d, 1-11 days after the first injection.

Fig. 2. Comparison of response latency (A) and the number of jumps (B) between the VEH and RES groups in response to the hot-plate test (a thermal stimulus) 3 days after the first injection.

****, $p < 0.0001$ (A: Welch's test; B: Mann-Whitney U test). Open circles, VEH group; filled circles, RES group. Numbers in parentheses indicate the number of animals.

Fig. 3. Comparison of the immobility time between the VEH and RES groups in the forced swim test on day 4 (A) and day 11 (B) after the first injection.

* $p < 0.05$ (Mann-Whitney U test). Open circles, VEH group; filled circles, RES group. Numbers in parentheses indicate the number of animals.

Fig. 4. Photomicrographs of the mice S1 in the VEH (A) and RES (B) groups.

Insets in “a” are shown in “b” as enlarged views. The number of PV-positive neurons was increased in the RES group. S1HL, S1 hindlimb area; S1FL, S1 forelimb area

Fig. 5. Comparison of the PV-positive neuron density in the S1FL (A), S1HL (B), and S1L (C) between the VEH and RES groups.

S1FL, S1 forelimb area; S1HL, S1 hindlimb area; S1L, S1 leg area (mean of S1FL and S1HL). ***, $p < 0.001$ (Welch's test). Open circles, VEH group; filled circles, RES group. Numbers in parentheses indicate the number of animals.

Fig. 6. Relationships between response latency in the hot-plate test and PV-positive neuron density in the S1FL (A), S1HL (B), and S1L (C).

*, **, $p < 0.05$, 0.01, respectively. Open circles, VEH group; filled circles, RES group. Other descriptions are shown in Fig. 5.

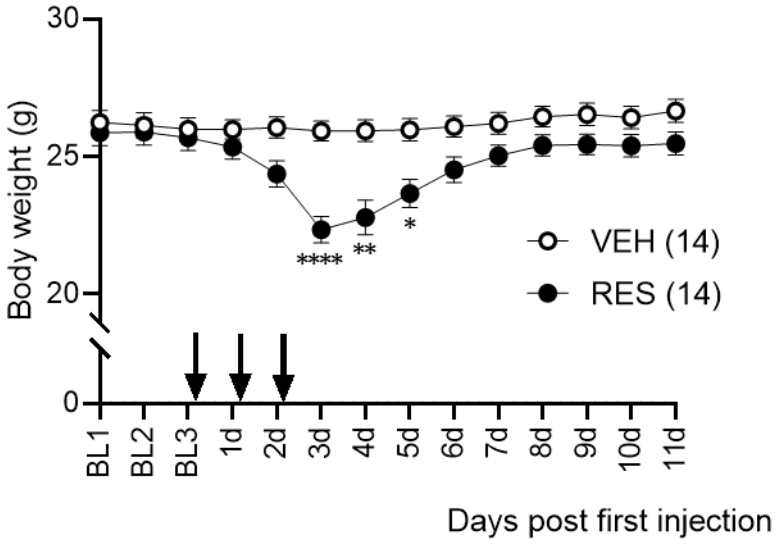
30
25
20
0
Body weight (g)
****
**
*
VEH (14)
RES (14)
BL1
BL2
BL3
1d
2d
3d
4d
5d
6d
7d
8d
9d
10d
11d
Days post first injection

Fig.1

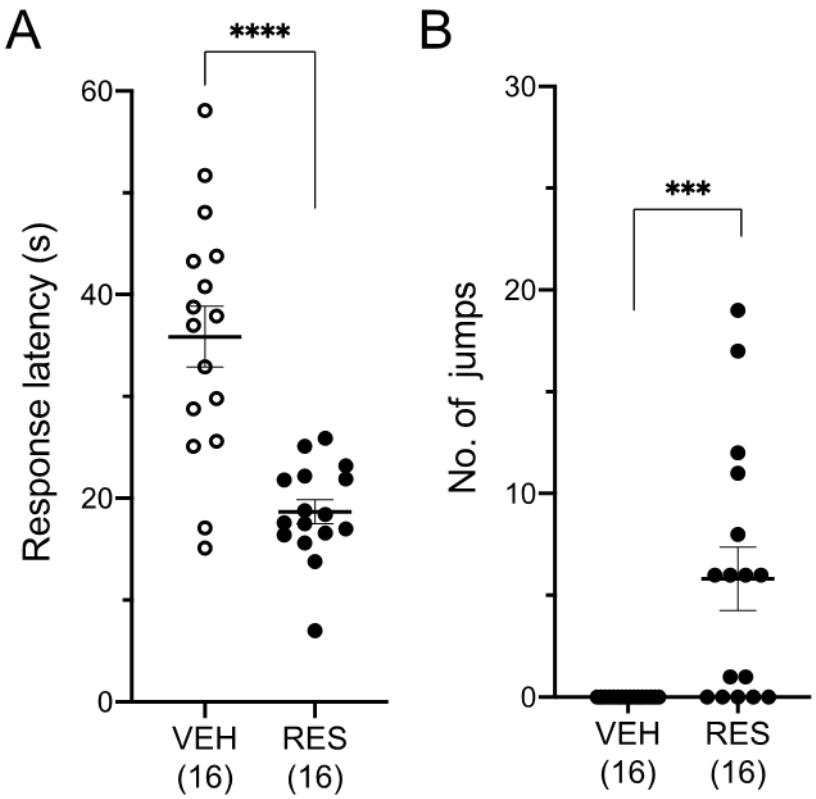
A
****
60
40
20
0
Response latency (s)
VEH
(16)
RES
(16)
B
***
30
20
10
0
No. of jumps
VEH
(16)
RES
(16)

Fig.2

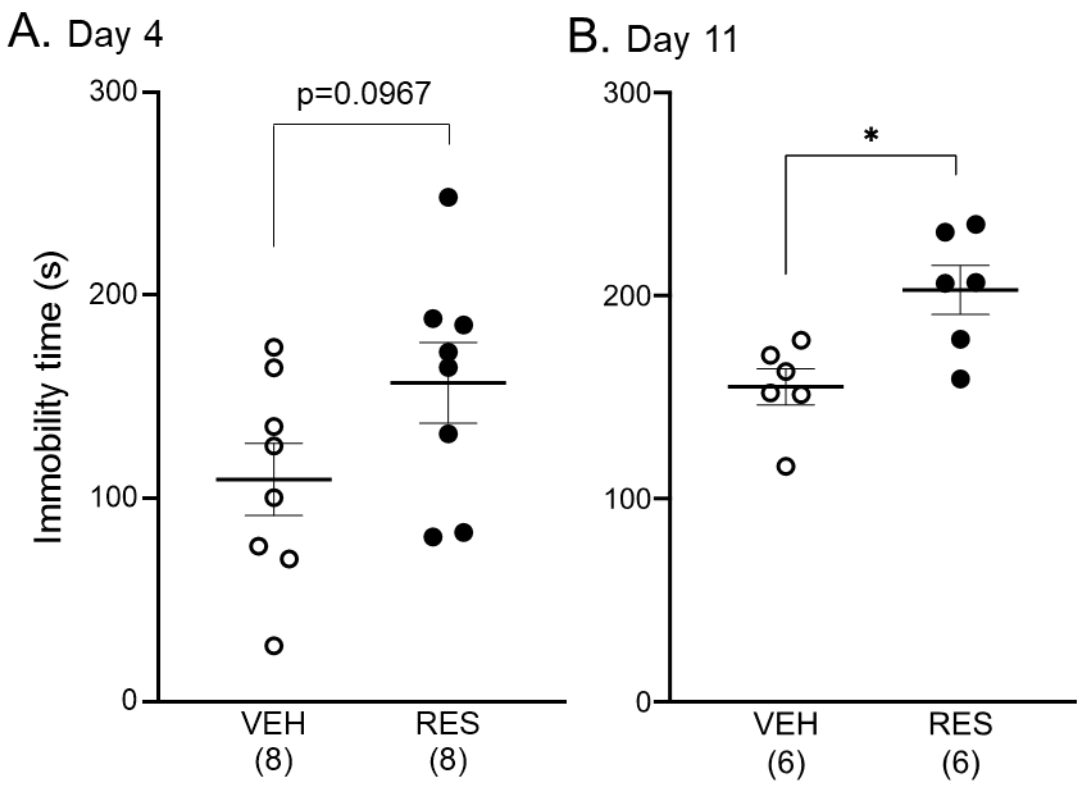
A. Day 4
p=0.0967
300
200
100
0
Immobility time (s)
VEH
(8)
RES
(8)
B. Day 11
*
300
200
100
0
VEH
(6)
RES
(6)

Fig.3

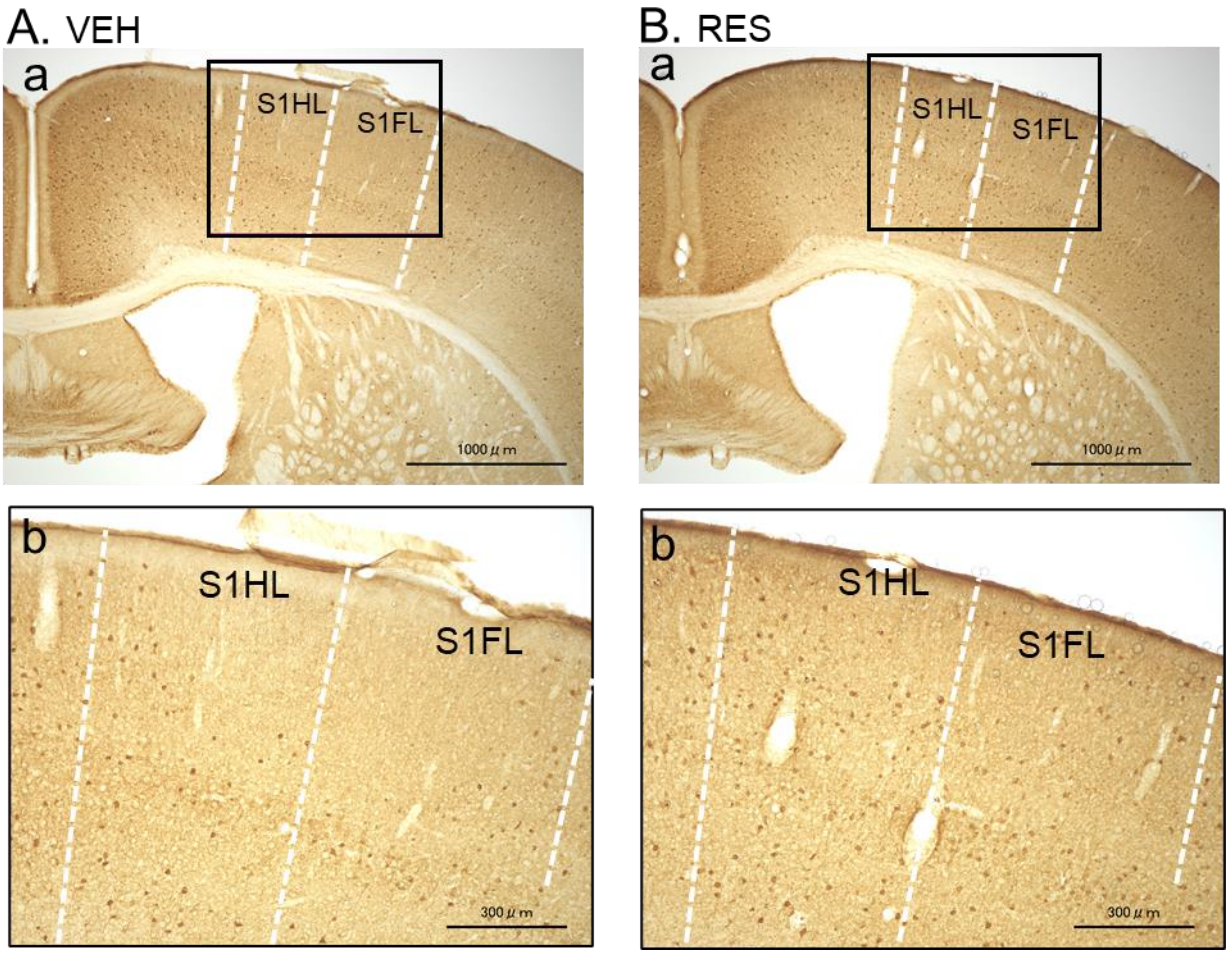
A. VEH
a
S1HL
S1FL
1000 μm
B. RES
a
S1HL
S1FL
1000 μm
b
S1HL
S1FL
300 μm
b
S1HL
S1FL
300 μm

Fig.4

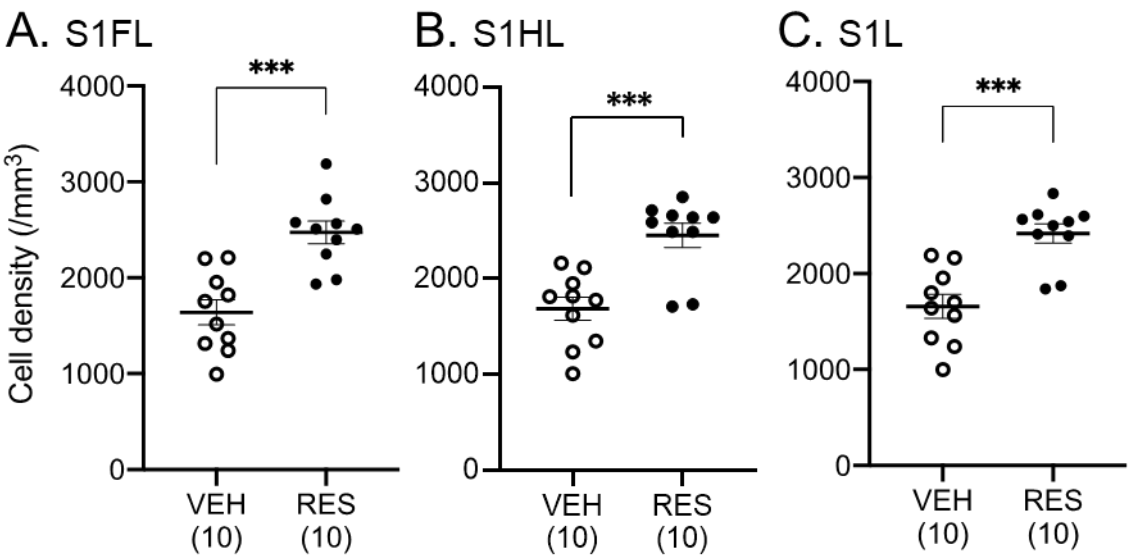
A. S1FL
B. S1HL
C. S1L
Cell density (/mm3)
4000
3000
2000
1000
0
***
VEH
(10)
RES
(10)

Fig.5

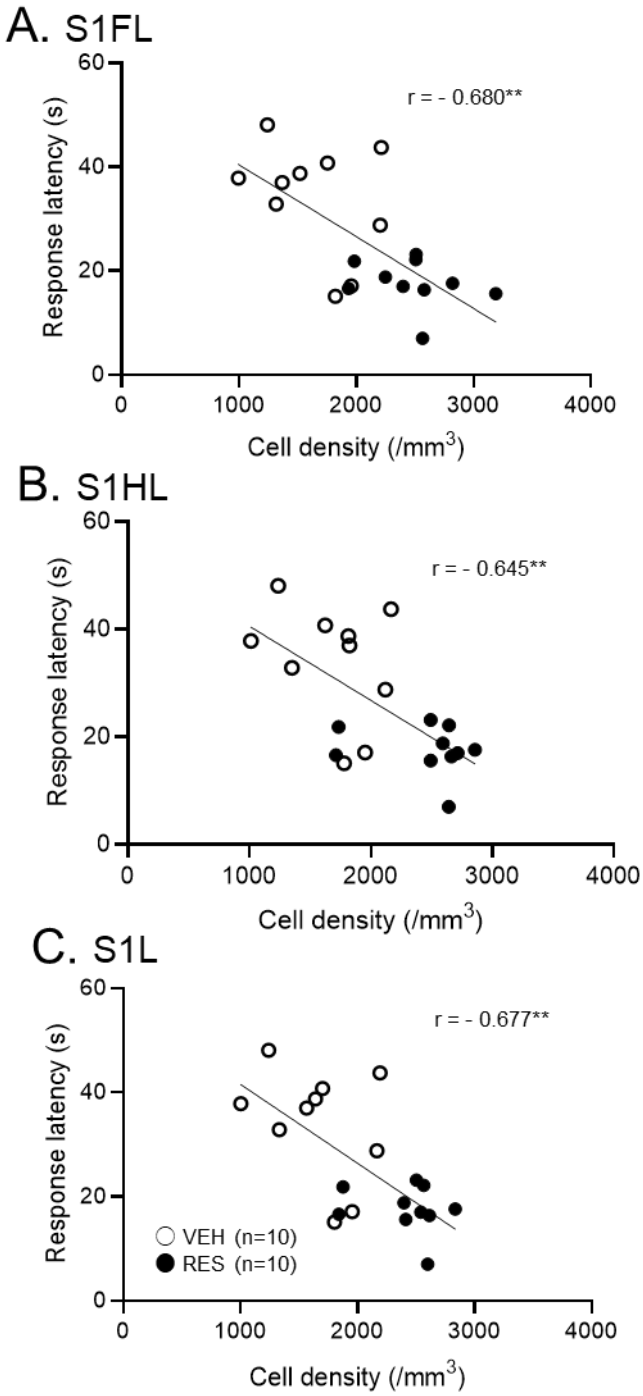

Fig.6

Supplementary figures

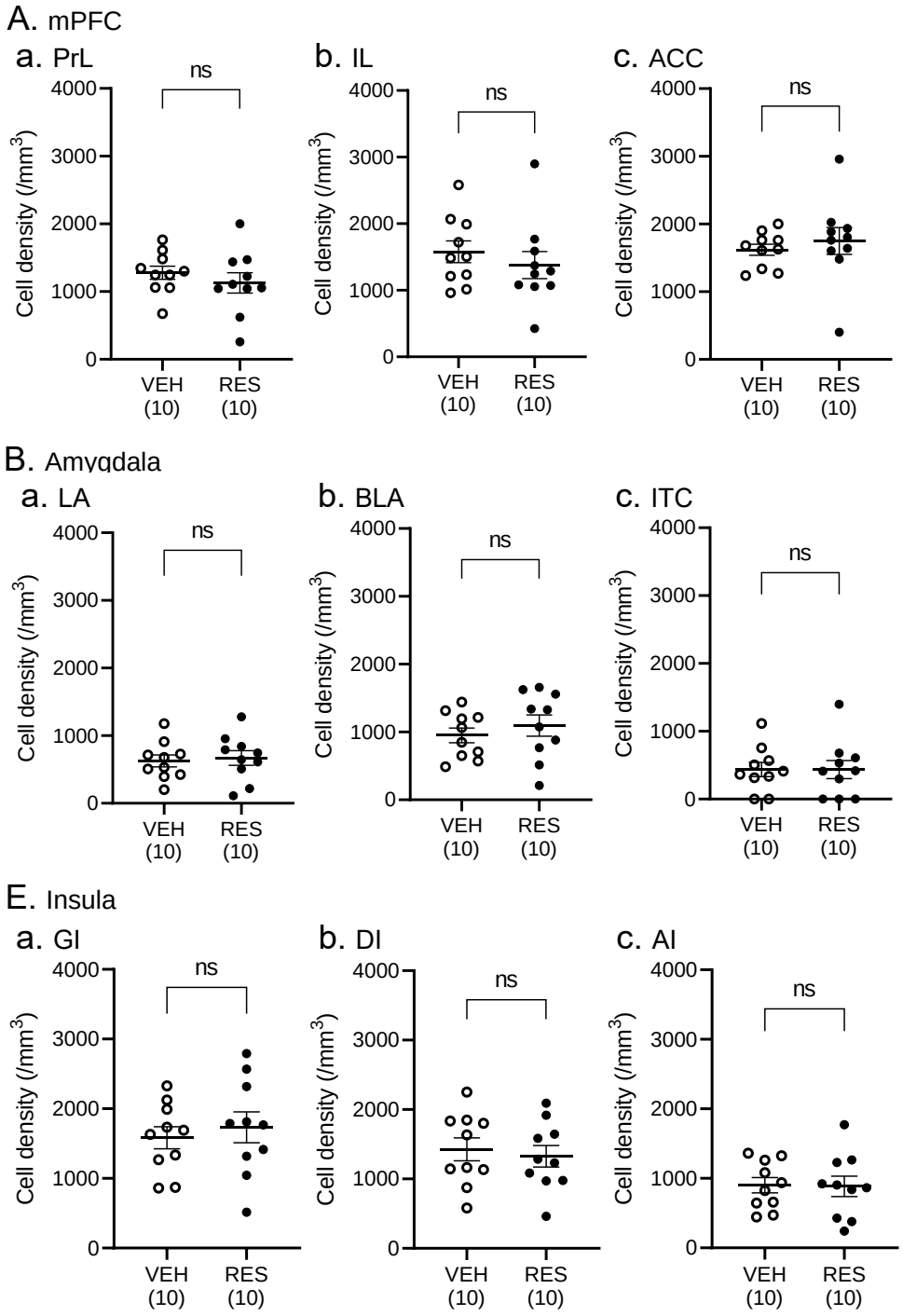

Supplementary Fig. 1. Comparison of the cell density of PV-positive neurons between the VEH and RES groups in the medial prefrontal cortex (mPFC) (A), amygdala (B), and insula (C).

There were no significant differences in the PV-positive neuron density between the VEH and RES groups in all regions (Mann-Whitney U test, $p > 0.05$). Numbers in parentheses indicate the number of animals. ns, non-significant ($p > 0.05$); PrL, prelimbic cortex; IL, infralimbic cortex; ACC, anterior cingulate cortex; LA, lateral nucleus of the amygdala; BLA, basolateral nucleus of the amygdala; ITC, intercalated cells in the amygdala; GI, granular insula; DI, dysgranular insula; AI, agranular insula.

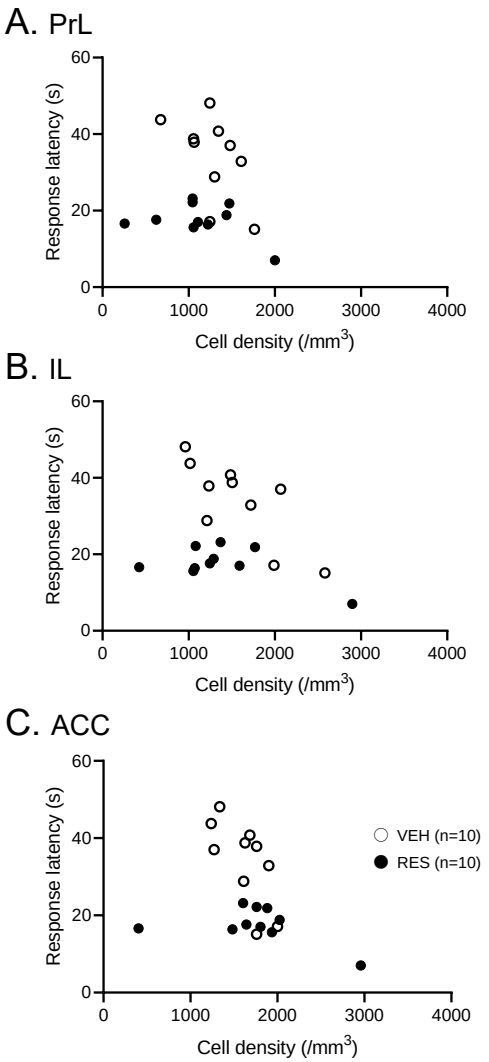

Supplementary Fig. 2. Relationship between the response latency in the hot-plate test and PV-positive neuron density in the prelimbic cortex (PrL) (A), infralimbic cortex (IL), and anterior cingulate cortex (ACC).
There was no significant correlation between response latency and PV-positive neuron density in the PrL [r = -0.128; F(1, 18)=1.638, p = 0.297], IL [r = -0.289; F(1, 18)=0.299, p = 0.297], and ACC [r = -0.376; F(1, 18)=2.245, p = 0.151].

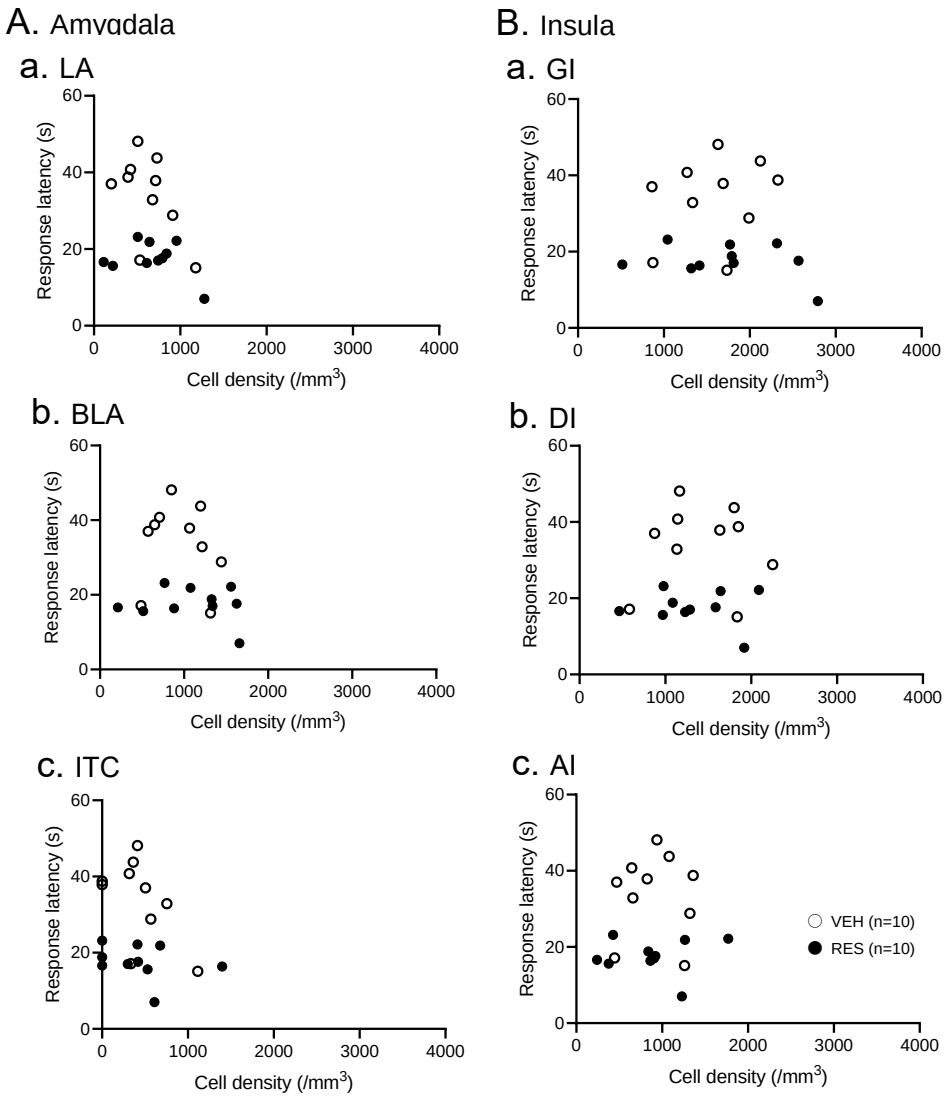

Supplementary Fig. 3. Relationships between response latency in the hot-plate test and PV-positive neuron density in the lateral nucleus (LA) (a), basolateral nucleus (BLA) (b), intercalated cells (ITC) (c) of the amygdala (A), and the granular insula (GI) (a), dysgranular insula (DI) (b), and agranular insula (AI) (c) of the insula cortex (B).

There were no significant correlations between the response latency and PV-positive neuron density in the LA [r = -0.333; F(1, 18)=2.958, p = 0.103], BLA [r = -0.215; F(1, 18)=0.872, p = 0.663], ITC [r = -0.269; F(1, 18)=1.404, p = 0.251], GI [r = -0.069; F(1, 18)=0.086, p = 0.773], DI [r = 0.075; F(1, 18)=0.101, p = 0.754], and AI [r = 0.030; F(1, 18)=0.016, p = 0.900].